3D-QSAR CoMFA and CoMSIA studies for design of potent human steroid 5 alpha-reductase inhibitors

ARTICLE *in* MEDICINAL CHEMISTRY RESEARCH · JANUARY 2012

Impact Factor: 1.4 · DOI: 10.1007/s00044-012-0006-1

2 AUTHORS:

Rajnish Kumar
Karolinska Institutet
20 PUBLICATIONS **50** CITATIONS
SEE PROFILE

Manoj Kumar
King George's Medical University
16 PUBLICATIONS **197** CITATIONS
SEE PROFILE

3D-QSAR CoMFA and CoMSIA studies for design of potent human steroid 5α-reductase inhibitors

Rajnish Kumar & Manoj Kumar

Medicinal Chemistry Research

ISSN 1054-2523

Med Chem Res
DOI 10.1007/s00044-012-0006-1

Springer

Med Chem Res
DOI 10.1007/s00044-012-0006-1

MEDICINAL CHEMISTRY RESEARCH

ORIGINAL RESEARCH

3D-QSAR CoMFA and CoMSIA studies for design of potent human steroid 5α-reductase inhibitors

Rajnish Kumar · Manoj Kumar

Received: 30 December 2011 / Accepted: 24 February 2012

Abstract 3D-QSAR studies were performed on a set of sixty-one 6-azasteroidal human steroid 5α-reductase inhibitors. The models developed using comparative molecular field analysis (CoMFA) and comparative molecular similarity indices analysis (CoMSIA) methodologies employing atom and centroid based alignment were reliable and significant having good predictive r^2 value. CoMSIA model developed by a combination of steric, electrostatic, hydrophobic and hydrogen bond donor showed good relative and predictive properties. The predictive power of the models was assessed using an external test set of 10 compounds. The best model had shown cross validation r^2 (0.702) with 7 optimum components, non-cross-validation r^2 (0.956), F value (86.158), predicted r^2 (0.704), standard error of estimate (0.165). Further the CoMFA/CoMSIA contour plots show a preference toward the C-17 substituents and indicate that bulky group at C-17 is an important requirement for exhibiting 5α-reductase inhibition. These developed models could be used to design and optimise the more potent 6-aza steroidal inhibitors of 5α-reductase enzyme.

Keywords Testosterone · Dihydrotestosterone · BPH · 3D-QSAR · 5α-reductase

Introduction

Benign prostatic hyperplasia (BPH) is a progressive, non-malignant disorder of the prostate in men aged 50 years or older. The term 'BPH' actually refers to a histological condition, namely the presence of stromal-glandular hyperplasia within the prostate gland (Emberton *et al.* 2008). It is characterised by an enlarged prostate (≥30 ml), lower urinary tract symptoms (LUTS), and decreased flow rate of urine (Q_{max}) (<15 ml/s) (Marberger 2006). LUTS in association with the prostatic enlargement affects 25% of the male population, increasing to about 43% of men over 60 (McNicholas and Mitchell 2008). As estimated 75% of men >50 years of age have symptoms arising from the BPH and 20–30% of men reaching 80 years of age require surgical intervention for the management of BPH (Parsons and Kashefi 2008; Roehrborn *et al.* 2009). Although the pathogenesis/molecular trigger of BPH is not fully understood, several mechanisms seem to be involved in the development and progression of the disease. These mainly include systemic and local hormonal and vascular alterations as well as prostatic inflammation that would stimulate cellular proliferation (Briganti *et al.* 2009). Chronic prostatic inflammation may result from the immunologic response of different pathogen noxae that induce tissue damage and subsequent chronic processes of repetitive wound healing, and it may have a role in BPH growth and progression as well as in the prostate's vulnerability to developing cancer (De Nunzio *et al.* 2011). The obstructive symptoms of BPH (straining, hesitancy, a weak stream, intermittency, a sense of incomplete emptying and terminal dribbling) reflects the effect of mechanical obstructions, while the irritative symptoms (urgency, frequency and nocturia) results from the uninhibited detrusor urinae muscle contractions (Barry and Roehrborn 1997).

Dihydrotestosterone (DHT) is the primary androgen that is responsible for prostate growth. The biological source of DHT is testosterone that is irreversibly reduced by the NADPH dependent human 5α-reductase (EC 1.3.99.5) in

R. Kumar · M. Kumar (✉)
University Institute of Pharmaceutical Sciences,
Panjab University, Chandigarh 160014, India
e-mail: manoj_uips@pu.ac.in

Published online: 17 March 2012

skin and prostate tissues (Fig. 1). Two types of isoforms of this enzyme, type 1 and type 2 were identified using human and rat prostatic complimentary deoxyribose nucleic acid (cDNA) libraries. Among these two isoforms, type 2 is mainly located in the prostate tissue, while type 1 is found in the periphery (Andersson and Russell 1990). Recently a third type of 5α-reductase enzyme (type 3) has been identified in hormone refractory prostate cancer cells (HRPC), which is located on SRD5A2L gene and converts testosterone into DHT in a similar way to type 1 enzyme (Aggarwal *et al*. 2010c; Uemura et al. 2008). Both of the isozymes 1 and 2 are expressed in normal prostate tissue but overexpressed in BPH where they are responsible for the hyperplasia of stromal and epithelial cells in the transition zone and periurethral glands of the prostate that results in prostate gland enlargement. Currently two structurally similar drugs are available for the clinical management of BPH i.e. finasteride and dutasteride (Fig. 2). Dutasteride is a dual 5α-reductase inhibitor that inhibit both type 1 and type 2 isozymes while finasteride is type 2 inhibitor. Dutasteride induces a more profound reduction of serum DHT in the range of 90-95% compared with 70-75% for finasteride due to its dual inhibition pattern (Gravas and Oelke 2010).

Quantitative structure activity relationship (QSAR) studies are generally used for generation of mathematical models to correlate biological activity and structural elements of the molecules under study. The basic assumption behind this is that variation of biological activity within a series can be correlated with changes in measured or computed molecular features. Further QSAR studies are popular due to their manifold contributions in drug design in account of saving time, money and human resources. Lack of knowledge about crystal structure of the isozymes is the major hurdle in the discovery of novel 5α-reductase inhibitors (5ARIs). Thus ligand based drug designing approaches like pharmacophore mapping and QSAR studies are few tools available for rational design of potent 5ARIs. Several 3D-QSAR studies have been reported from our laboratory focused on refining the molecular architecture essential for inhibition of 5α-reductase enzyme using Self Organising Molecular Field Analysis (SOMFA) (Aggarwal *et al*. 2010a, b; Aggarwal *et al*. 2011; Thareja *et al*. 2009). In continuation of our efforts to optimise the structural requirements for potent 5ARIs, we have carried out 3D-QSAR studies on a series of substituted 6-azasteroidal derivatives as 5ARIs. The present study includes comparative molecular field analysis (CoMFA) and comparative

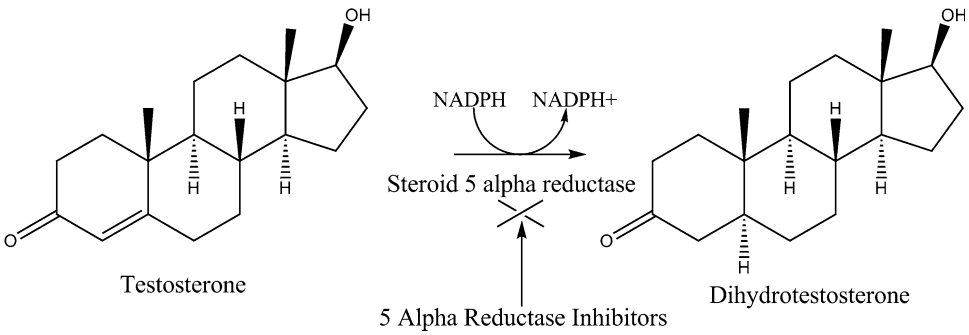

Fig. 1 Inhibition of enzyme 5α-reductase which catalyses the conversion of testosterone into the more active dihydrotestosterone using NADPH as a cofactor

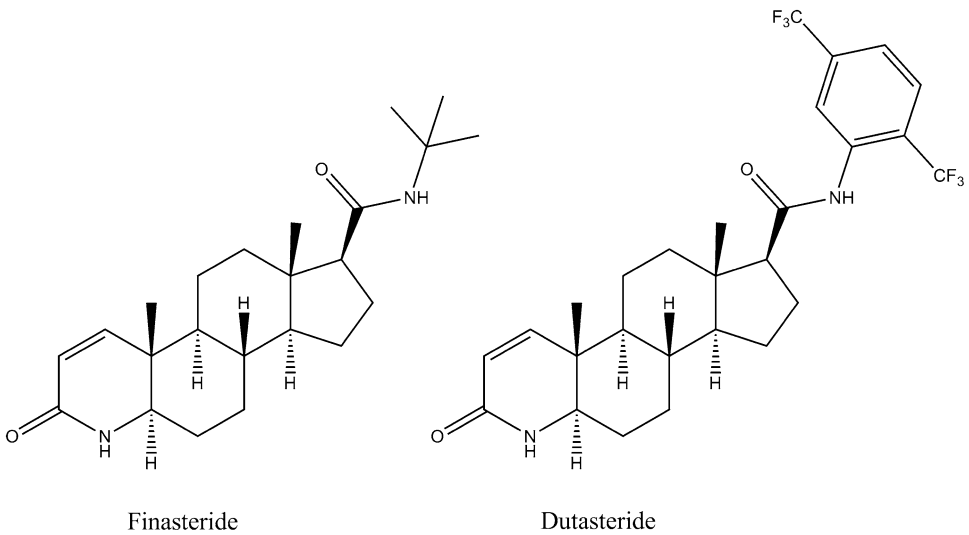

Fig. 2 Clinically available 5α-reductase inhibitors used for the management of BPH

molecular similarity indices analysis (CoMSIA) methodologies. Atom and centroid based alignment method was used for alignment of the database over lowest energy conformation of the most active compound as a template. The refined 3D QSAR models could be used to get a better insight for design and optimisation of potent 5ARIs.

Methods

Data set for CoMFA and CoMSIA analysis

For a valid model it is required that the dataset used should cover the evenly distributed biological activity in a range of at least 2–3 orders of magnitude. Taking this into consideration 61 molecules were selected for the present study from the published work of Frye *et al.* (1993, 1994, 1995). The biological activity used in the present study was expressed as pIC_{50} where, pIC_{50} is the negative logarithm of molar concentration in nanomoles of the inhibitors producing 50% inhibition of 5α-reductase type 2 enzyme. The dataset was divided into a training set of 51 molecules and a test set of 10 molecules which were used to assess the predictivity of the models. The test set was judiciously chosen so that it covered almost entire range of biological activity and structural diversity. The general structure of the test and training set molecules along with the obtained and predicted activity have been presented in Tables 1, 2, 3, 4.

Table 1 Compounds (**1–19**) used in the 3D QSAR study

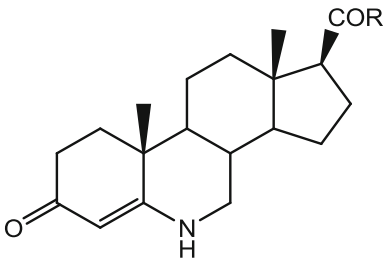

Comp. no.	R	Biological activity			
		Observed		Predicted (CoMSIA)	Residual
		IC_{50} (nM)	pIC_{50}	pIC_{50}	
1	OCH_3	3.2	−0.5051	−0.592	0.0871
2	O-2-adamantyl	0.04	1.3979	1.364	0.0337
3	NMeOMe	2.4	−0.3802	−0.333	−0.0476
4	NH-1-adamantyl	0.07	1.1549	0.851	0.3037
5	N-i-pr_2	0.36	0.4437	0.541	−0.0976
6	NH-i-pr	6.7	−0.8261	−0.416	−0.4105
7	NMeEt	2.8	−0.4472	−0.177	−0.2701
8	$NHCH_2Ph$	0.58	0.2366	0.109	0.1273
9	$N(CH_2Ph)_2$	0.13	0.8861	0.873	0.0133
10	$NHCHPh_2$	0.09	1.0458	1.07	−0.0241
11^T	$NHCPh_3$	0.09	1.0458	0.875	0.1713
12	$NHCH(4\text{-fluorophenyl})_2$	0.16	0.7959	0.794	0.0021
13	$NHCH(4\text{-chlorophenyl})_2$	0.12	0.9208	0.929	−0.0085
14	$NHCH(cyclohexyl)_2$	0.40	0.3979	0.343	0.0547
15	$NHNPh_2$	0.23	0.6383	0.64	−0.0013
16^T	Piperazine	33	−1.5185	−0.625	−0.8936
17	Morpholine	7.1	−0.8513	−0.765	−0.0864
18	Thiomorpholine	1.3	−0.1139	−0.046	−0.0682
19	i-Bu	0.08	1.0969	1.08	0.0165

T test set molecule

Table 2 Compounds (**20–23**) used in the 3D QSAR study

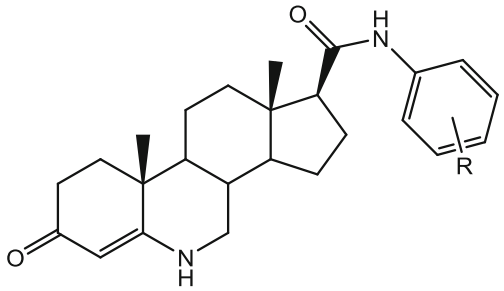

Comp. no.	R	Biological activity			Residual
		Observed		Predicted (CoMSIA)	
		IC_{50} (nM)	pIC_{50}	IC_{50} (nM)	
20	–	1.4	−0.1461	−0.132	−0.0143
21^{T}	2-*t*-butyl	0.2	0.6990	1.166	−0.4674
22	2-(4-*t*-butylphenyl), 5-trifluoromethyl	0.5	0.3010	0.253	0.0483
23	3,5-bis(trifluoromethyl)	0.2	0.6990	0.712	−0.0126

T test set molecule

Computational approach and molecular alignment

Molecular modelling, CoMFA and CoMSIA analysis were performed using SYBYL 7.0 and SYBYL-X software (SYBYL Molecular Modeling System 2003). Structures of all the compounds were built using the most active compound as template in SYBYL. The partial charges for all of the compounds were calculated using Gasteiger–Huckel method. The geometry of the molecules was optimised using Tripos force field with a distance dependent dielectric function and energy convergence criterion of 0.001 kcal/mol Å with standard SYBYL settings and keeping maximum 1,000 iterations. In 3D-QSAR studies, determination of biologically active conformation and molecular alignment of the compounds are the most important factors that affects quality of the model. The positioning of the molecular model within the fixed lattice is an important input variable in CoMFA, since the relative interaction energies depend strongly on the relative molecular positions (Cramer *et al*. 1988). In the current study atoms and centroids-based alignment was used to superimpose the molecules over the most active one. The SYBYL conventional fit atom alignment rule was applied. The atom based alignment module adjusts the geometry in such a way that its steric and electrostatic fields matched the template molecule (Murumkar *et al*. 2011). Commonly template molecule is selected among; (a) the most active molecule (b) lead molecule (c) molecule containing the largest number of functional groups. Taking this into consideration, compound (**2**) was selected as the template molecule, which was most potent inhibitor of the enzyme 5α-reductase among the series. The lowest energy conformer of the compound was obtained using Multisearch option in SYBYL. The atoms (Centroid C1, C2 and atom *) used for alignment of the compounds under study were as shown in Fig. 3. Superimposition of all the molecules under study on the template has been shown in Fig. 4.

CoMFA methodology

The steric (Lennard-Jones potential) and electrostatic fields (Coulombic potentials) were calculated at each lattice intersection for the aligned molecules kept in a 3D cubic lattice with a grid spacing of 2.0 Å in x, y and z coordinates. The van der Waals and Coulombic potential terms representing the steric and electrostatic fields, respectively, were calculated using standard Tripos force fields. A sp^3 carbon atom having a charge of +1 and a radius of 1.52 Å was used as a probe to calculate the steric and electrostatic fields. The steric and electrostatic fields were truncated at 0.3 kcal mol^{-1}. The other parameters were used as default because, the effect of altering the lattice spacing, column filtering and energy cut off values in the CoMFA process appears to be minimal and thus the use of the default settings for these parameters seems appropriate (Mittal *et al*. 2009).

CoMSIA interaction energy calculation

In CoMSIA interaction energy calculation, the steric, electrostatic, hydrophobic, hydrogen bond donor and

Table 3 Compounds (**24–43**) used in the 3D QSAR study

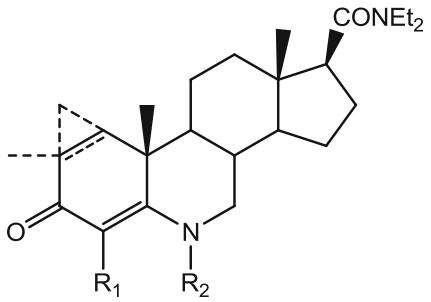

Comp. no.	R_1	R_2	Others	Biological activity			Residual
				Observed		Predicted (CoMSIA)	
				IC_{50} (nM)	pIC_{50}	IC_{50} (nM)	
24	H	H	–	1.5	−0.1761	−0.161	−0.0156
25	H	H	Δ^1	3.5	−0.5441	−0.396	−0.148
26	H	H	1,2-α Methano	1.8	−0.2553	−0.25	−0.0057
27	H	H	2 α,β-Me	3.4	−0.5315	−0.483	−0.0488
28^T	H	CN	–	42	−1.6232	−0.515	−1.1078
29	H	Me	–	2.3	−0.3617	−0.426	0.0643
30	H	Et	–	3.5	−0.5441	−0.54	−0.0037
31	H	Pr	–	4.2	−0.6232	−0.913	0.2896
32^T	H	i-Pr	–	4.9	−0.6902	−0.768	0.0778
33	H	Bu	–	29	−1.4624	−1.173	−0.2895
34	H	Hex	–	12	−1.0792	−1.226	0.1465
35	H	Bn	–	40	−1.6021	−1.62	0.0175
36	H	Me	Δ^1	5.7	−0.7559	−0.872	0.1158
37^T	H	Me	1,2-α Methano	5	−0.6990	−0.689	−0.0095
38	Cl	H	–	1.9	−0.2788	−0.424	0.1453
39	Br	H	–	2.1	−0.3222	−0.569	0.2464
40	I	H	–	6.0	−0.7782	−0.841	0.0624
41	Me	H	–	3.9	−0.5911	−0.372	−0.219
42	Me	H	Δ^1	8.1	−0.9085	−0.885	−0.0233
43^T	Me	Me	–	4.5	−0.6532	−0.425	−0.2284

T test set molecule

hydrogen bond acceptor potential fields were calculated at each lattice intersection of the same lattice box used for CoMFA calculations (Klebe *et al*. 1994). In the present study, standard settings of CoMSIA (probe with charge +1, radius 1 Å and hydrophobicity +1, attenuation factor of 0.3 and grid spacing 2 Å) were used to calculate the steric, electrostatic, hydrophobic, donor and acceptor fields.

Partial least square (PLS) analysis

PLS method (Puntambekar et al. 2006) was used to correlate 5α-reductase inhibitory activity with the CoMFA and CoMSIA fields to derive 3D-QSAR models. Cross validation analysis was performed internally using leave one out (LOO) method in which one compound is removed from the dataset and its activity is predicted using the model derived from the rest of the dataset (Kumar *et al*. 2011). The cross validation r^2 that resulted in optimum numbers of components and lowest standard error of prediction were considered for further analysis. The external validation of various models was performed using a test set of 10 molecules. The analysis was carried out with the column filtering value of 2.0 kcal/mol to speed up the calculation and reduce the noise. Final analysis was performed to calculate non cross validated r^2 using the optimum number of components. The cross validation r^2, Fischer's statistic (F-test), Standard error of estimate and predicted r^2 were calculated.

Table 4 Compounds (**44–61**) used in the 3D QSAR study

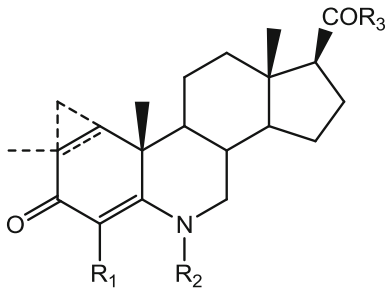

Comp. no.	R_1	R_2	R_3	Others	Biological activity			Residual
					Observed		Predicted (CoMSIA)	
					IC_{50} (nM)	pIC_{50}	IC_{50} (nM)	
44[T]	H	H	NH-*t*-Bu	–	0.88	0.0555	−0.244	0.3
45	H	H	NH-*t*-Bu	Δ^1	1.8	−0.2553	−0.417	0.1612
46	H	H	NH-*t*-Bu	1,2-α methano	4.4	−0.6435	−0.411	−0.2322
47	H	Me	NH-*t*-Bu	–	1.7	−0.2304	−0.479	0.2486
48	H	Me	NH-*t*-Bu	Δ^1	6.7	−0.8261	−0.68	−0.146
49	Me	H	NH-*t*-Bu	–	1.4	−0.1461	−0.249	0.1024
50	Me	Me	NH-*t*-Bu	–	8.6	−0.9345	−1.052	0.1175
51[T]	H	Me	i-Bu	–	0.10	1	0.637	0.3627
52	Br	H	i-Bu	–	0.40	0.3979	0.438	−0.04
53	H	Me	NH-1-Ad	–	0.30	0.5229	0.596	−0.073
54	Br	Me	NH-1-Ad	–	1.7	−0.2304	0.084	−0.3145
55	Me	Me	NH-1-Ad	–	0.4	0.3979	0.231	0.1672
56	H	Me	$NHCHPh_2$	–	0.20	0.6990	0.782	−0.0832
57[T]	H	Pr	$NHCHPh_2$	Δ^1	1.3	−0.1139	0.131	−0.0174
58	H	H	Piperidine	–	0.50	0.3010	0.24	0.0613
59	H	H	NOH-*t*-Bu	–	0.60	0.2218	0.238	−0.0163
60	H	H	*n*-Pr	–	0.30	0.5229	0.452	0.0707
61	H	H	2,4,6-triisopropyl phenyl	–	0.50	0.3010	0.305	−0.0035

T test set molecule

Results and discussion

CoMFA and CoMSIA analysis were used to develop QSAR models on a set of sixty-one 6-azasteroidal 5ARIs. The lowest energy conformation of all the compounds were obtained and considered for database alignment. Due to unavailability of crystal structure of the enzyme and the co-crystallized ligand, the lowest energy conformer of the most active compound (**2**) was used as a template molecule for the purpose of alignment. Various models were developed using CoMFA and CoMSIA fields. The developed models were predicted externally using a test set of 10 molecules. The models with significant predictive and correlative power are reported in Table 5. The predicted and residual activity of the compounds obtained using the best model is given in Tables 1, 2, 3, 4. The plot between observed and predicted activities of test and training set is shown in Fig. 5.

CoMFA analysis

The negative logarithm of IC_{50} (pIC_{50}) was used as the dependent variable and is given in Tables 1, 2, 3, 4. The CoMFA models were built using a training set of fifty one molecules and tested against a test set of ten molecules. The selection of training set and test set was done by considering the structural diversity and the range of biological activity. The energy minimised structures of all the compounds were aligned using atom/centroid based alignment method. The minimum energy conformation of the most active compound (**2**) was used as a template molecule. PLS analysis was carried out using column filtering value of 2.0 kcal/mol. The CoMFA

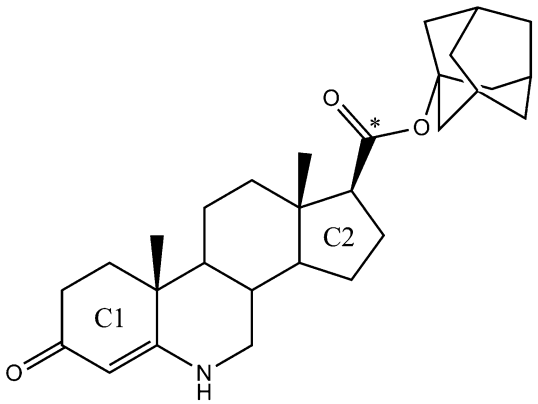

Fig. 3 Designation of centroids (C1 and C2) and atom (*asterisk*) for alignment shown in template molecule

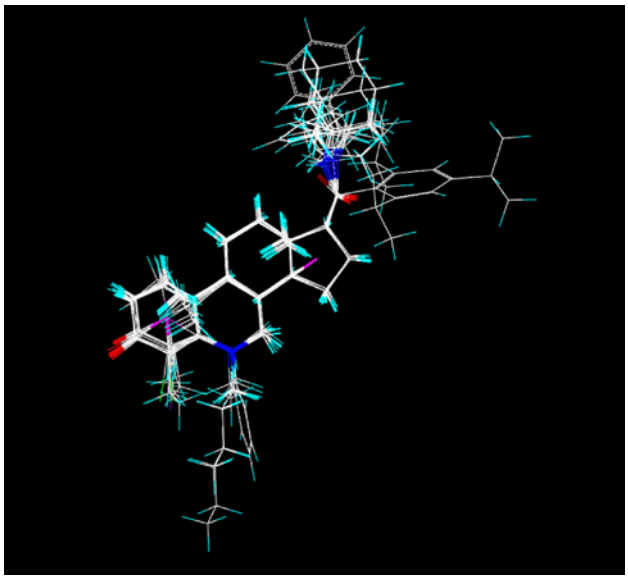

Fig. 4 Atom and centroid based alignment of the molecules used in CoMFA and CoMSIA analysis

model showed cross validation $r^2 = 0.536$ with 3 optimum components, non-cross-validation $r^2 = 0.899$, F value = 65.219, predicted $r^2 = 0.507$, standard error of estimate (SEE) = 0.246; the steric and electrostatic contributions were 77.8 and 22.2%, respectively. In CoMFA and CoMSIA study predicted r^2 value of >0.3 is considered as statistically significant but a value of >0.5 can be considered as statistically more significant (Bohm *et al.* 1999). The developed model was found to be statistically significant towards describing the 5α-reductase inhibitory activity due to its high non-cross-validation r^2 and low standard error of estimate.

CoMSIA analysis

The CoMSIA analysis was performed using steric, electrostatic, hydrophobic, hydrogen bond donor and hydrogen bond acceptor fields. Various models were developed using a combination of different fields and the statistically significant three models are reported here as in Table 5. The CoMSIA

Table 5 PLS statistics of CoMFA and CoMSIA models

Parameter	CoMFA	COMSIA		
		SEHDA	SEHD	SEHA
r^2_{cv}	0.536	0.685	**0.702**	0.614
ONC	3	8	**7**	4
r^2_{ncv}	0.899	0.955	**0.956**	0.957
SEE	0.246	0.166	**0.165**	0.163
F-Value	65.219	85.625	**86.158**	88.788
r^2_{Pred}	0.507	0.547	**0.704**	0.572
Contribution (%)				
Steric (S)	77.8	21.9	**21.4**	22.3
Electrostatic (E)	22.2	13.6	**25.3**	20.4
Hydrophobic (H)	–	34.2	**36.7**	39.7
Donor (D)	–	16.6	**16.5**	–
Acceptor (A)	–	13.8	–	17.7

r^2_{cv} cross-validated correlation coefficient, *ONC* optimum number of components from PLS analysis, r^2_{ncv} non-cross-validated correlation coefficient, *SEE* standard error of estimate, *F* Fischer statistic, r^2_{Pred} predictive correlation coefficient

Bold values: this model is the most significant and predictive

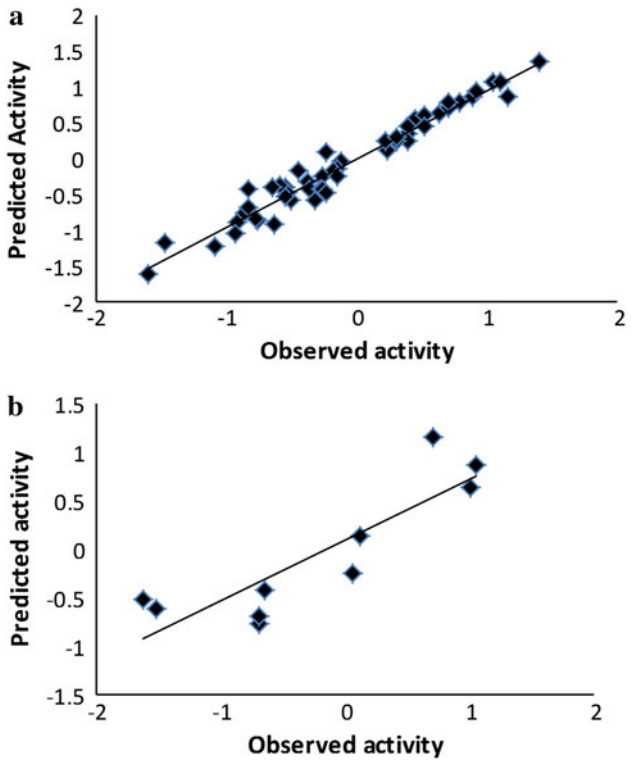

Fig. 5 Graph between observed and predicted activity for training set (**a**) and test set (**b**) molecules from the best predictive CoMFA (SEDH) model

Fig. 6 The CoMFA steric STDEV*COEFF contour plots of the most active compound (**2**). Sterically favoured areas (contribution level 80%) are represented by *green polyhedron*. Sterically disfavoured areas (contribution level 20%) are represented by *yellow polyhedron* (Color figure online)

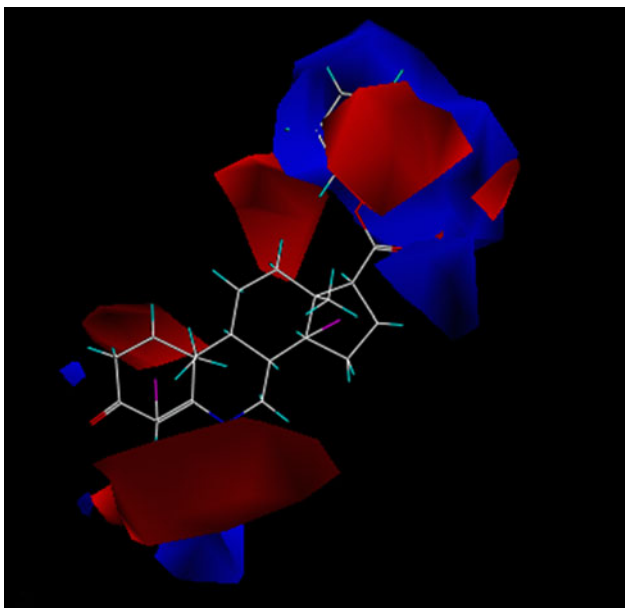

Fig. 7 The CoMFA electrostatic STDEV*COEFF contour plots of the most active compound (**2**). Positively charged favoured areas (contribution level 80%) are represented by *blue polyhedron*. Negatively charged favoured areas (contribution level 20%) are represented by *red polyhedron* (Color figure online)

model with combination of all the fields yielded a cross validation $r^2 = 0.685$ with 8 optimum components, non-cross-validation $r^2 = 0.955$, F value $= 85.625$, predicted $r^2 = 0.547$, SEE $= 0.166$; the steric, electrostatic, hydrophobic, hydrogen

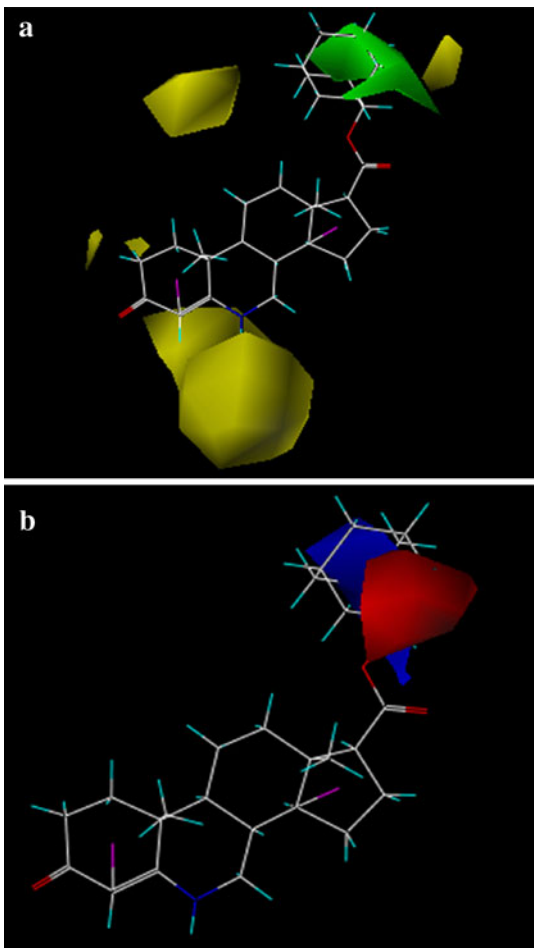

Fig. 8 The CoMSIA STDEV*COEFF contour plots of the most active compound (**2**). **a** Steric. **b** Electrostatic. *Yellow* and *green* contours show region where steric group is favoured and disfavoured the activity, respectively. *Blue* and *red* contours show region where positive charged substituent is favoured and negatively charged substituent is favoured the activity, respectively (Color figure online)

bond donor and hydrogen bond acceptor fields contribution were 21.9, 13.6, 34.2, 16.6 and 13.8% respectively. Combination of steric, electrostatic, hydrophobic and hydrogen bond donor fields yielded a CoMSIA model with cross validation $r^2 = 0.702$ with 7 optimum components, non-cross-validation $r^2 = 0.956$, F value $= 86.158$, predicted $r^2 = 0.704$, SEE $= 0.165$; the steric, electrostatic, hydrophobic and hydrogen bond donor fields contribution were 21.4, 25.3, 36.7 and 16.5% respectively. Combination of steric, electrostatic, hydrophobic and hydrogen bond acceptor fields yielded a CoMSIA model with cross validation $r^2 = 0.614$ with 4 optimum components, non-cross-validation $r^2 = 0.957$, F value $= 86.158$, predicted $r^2 = 0.704$, SEE $= 0.165$; the steric, electrostatic, hydrophobic and hydrogen bond donor fields contribution were 21.4, 25.3, 36.7 and 16.5%, respectively. The developed models were shown to be highly predictive as indicated by

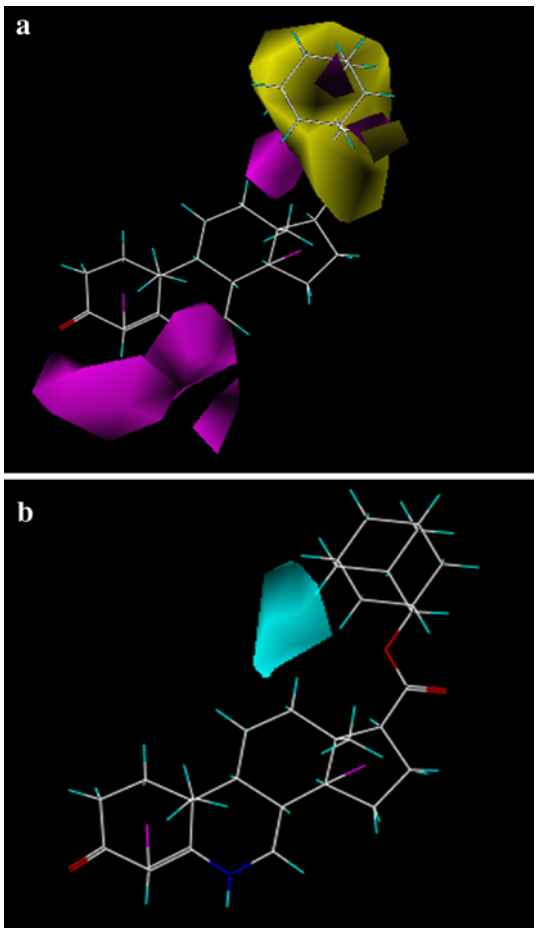

Fig. 9 The CoMSIA STDEV*COEFF contour plots of the most active compound (**2**). **a** Hydrophobic. **b** H-bond donor. *Yellow* and *purple* contours show region where hydrophobic group is favoured and disfavoured the activity, respectively. *Magenta* and *cyan* contours show region where H-bond donors are favoured and disfavoured the activity, respectively (Color figure online)

their robust statistical parameters given in Table 5. The major contributing field in CoMFA model was steric and in the case of CoMSIA, it was found to be steric as well as hydrophobic. The predicted and residual activities determined using the best model (CoMSIA SEHD) is given in Tables 1, 2, 3, 4.

CoMFA and CoMSIA contour maps

The CoMFA steric and electrostatic maps are shown in Figs. 6 & 7, respectively. In steric contour plots the sterically favoured areas are represented by green polyhedron. Sterically disfavoured areas are represented by yellow polyhedron. The green polyhedron shown near C-17 position indicates that the steric field is favourable at this position for activity while yellow colour at C-6 position indicated that steric bulk at this position disfavour the activity. In the case of electrostatic contour map (Fig. 7), blue colour region show area where electropositive groups enhances the activity, while red region represents the area where electronegative charge groups enhances the activity. It was found from the contour plot that substitution of electropositive groups near to C-17 position leads to enhanced activity while substitution of C-6 with electronegative groups enhances the activity. The CoMSIA steric and electrostatic contour plots with the compound (**2**) are shown in Fig. 8 (a) steric, (b) electrostatic and are similar to those obtained in CoMFA analysis. Figure 9 shows the contour plots with the compound (**2**) for; (a) Hydrophobic, (b) H-bond donor fields. Yellow and purple contours show region where hydrophobic group is favoured and disfavoured the activity, respectively. Magenta and cyan contours show region where H-bond donors are favoured and disfavoured the activity. It was found from the hydrophobic contour map that substitution at C-17 position with hydrophobic groups leads to increase in the activity, which indicates that the C-17 position substituents are responsible for hydrophobic interaction with the active site of the enzyme. It is in agreement with previously reported study which suggests that presence of hydrophobic groups at C-17 position of steroidal skeleton is useful for inhibitory activity and any substitution at C-6 position decreases the type-2 activity (Kurup *et al*. 2000). Further the results from present study could be used for design and optimisation of potent 5ARIs.

Conclusion

In the present study sixty-one 6-azasteroidal inhibitors of the enzyme 5α-reductase were selected for the development of 3D QSAR CoMFA and CoMSIA models. The selected molecules were subjected to atom and centroid based alignment over the minimum energy conformation of the most active compound from the series. The CoMFA model suggested high contribution of steric field for inhibition of 5AR. CoMSIA model developed with a combination of steric, electrostatic, hydrophobic and hydrogen bond donor fields showed better predictive ability for a test set of 10 compounds. Further the contribution of hydrophobic and steric field was found to be more thus indicating, steric and hydrophobic interaction of the inhibitors with the active site of enzyme. In conclusion several 3D-QSAR models were developed using CoMFA and CoMSIA methodologies which could be used for design and optimization of leads as 5ARIs.

Acknowledgments Authors are thankful to University Grant Commission (UGC), New Delhi, India for financial support (File No. 37-319/2009) (SR) and to MSU of Baroda for necessary help regarding computational work.

Declaration of interest The authors report no conflict of interest.

References

Aggarwal S, Thareja S, Bhardwaj TR, Kumar M (2010a) 3D-QSAR studies on unsaturated 4-azasteroids as human 5alpha-reductase inhibitors: a self organizing molecular field analysis approach. Eur J Med Chem 45(2):476–481

Aggarwal S, Thareja S, Bhardwaj TR, Kumar M (2010b) Self-organizing molecular field analysis on pregnane derivatives as human steroidal 5alpha-reductase inhibitors. Steroids 75(6): 411–418

Aggarwal S, Thareja S, Verma A, Bhardwaj TR, Kumar M (2010c) An overview on 5alpha-reductase inhibitors. Steroids 75(2):109–153

Aggarwal S, Thareja S, Verma A, Bhardwaj TR, Kumar M (2011) QSAR studies on human 5alpha-reductase inhibitors: unsaturated 3-carboxysteroids. Acta Pol Pharm 68(3):447–452

Andersson S, Russell DW (1990) Structural and biochemical properties of cloned and expressed human and rat steroid 5alpha-reductases. Proc Natl Acad Sci USA 87(10):3640–3644

Barry M, Roehrborn C (1997) Management of benign prostatic hyperplasia. Annu Rev Med 48:177–189

Bohm M, St rzebecher J, Klebe G (1999) Three-dimensional quantitative structure-activity relationship analyses using comparative molecular field analysis and comparative molecular similarity indices analysis to elucidate selectivity differences of inhibitors binding to trypsin, thrombin, and factor Xa. J Med Chem 42(3):458–477

Briganti A, Capitanio U, Suardi N, Gallina A, Salonia A, Bianchi M, Tutolo M, Di Girolamo V, Guazzoni G, Rigatti P, Montorsi F (2009) Benign prostatic hyperplasia and its aetiologies. Eur Urol Suppl 8(13):865–871

Cramer RD, Patterson DE, Bunce JD (1988) Comparative molecular field analysis (CoMFA). 1. Effect of shape on binding of steroids to carrier proteins. J Am Chem Soc 110(18):5959–5967

De Nunzio C, Kramer G, Marberger M, Montironi R, Nelson W, Schröder F, Sciarra A, Tubaro A (2011) The controversial relationship between benign prostatic hyperplasia and prostate cancer: the role of inflammation. Eur Urol 60(1):106–117

Emberton M, Cornel EB, Bassi PF, Fourcade RO, Gomez JM, Castro R (2008) Benign prostatic hyperplasia as a progressive disease: a guide to the risk factors and options for medical management. Int J Clin Pract 62(7):1076–1086

Frye SV, Haffner CD, Maloney PR, Mook RA Jr, Dorsey GF Jr, Hiner RN, Batchelor KW, Bramson HN, Stuart JD, Schweiker SL et al (1993) 6-Azasteroids: potent dual inhibitors of human type 1 and 2 steroid 5 alpha-reductase. J Med Chem 36(26):4313–4315

Frye SV, Haffner CD, Maloney PR, Mook RA Jr, Dorsey GF Jr, Hiner RN, Cribbs CM, Wheeler TN, Ray JA, Andrews RC et al (1994) 6-Azasteroids: structure-activity relationships for inhibition of type 1 and 2 human 5 alpha-reductase and human adrenal 3 beta-hydroxy-delta 5-steroid dehydrogenase/3-keto-delta 5-steroid isomerase. J Med Chem 37(15):2352–2360

Frye SV, Haffner CD, Maloney PR, Hiner RN, Dorsey GF, Noe RA, Unwalla RJ, Batchelor KW, Bramson HN, Stuart JD et al (1995) Structure-activity relationships for inhibition of type 1 and 2 human 5 alpha-reductase and human adrenal 3 beta-hydroxy-delta 5-steroid dehydrogenase/3-keto-delta 5-steroid isomerase by 6-azaandrost-4-en-3-ones: optimization of the C17 substituent. J Med Chem 38(14):2621–2627

Gravas S, Oelke M (2010) Current status of 5alpha-reductase inhibitors in the management of lower urinary tract symptoms and BPH. World J Urol 28(1):9–15

Klebe G, Abraham U, Mietzner T (1994) Molecular similarity indices in a comparative analysis (CoMSIA) of drug molecules to correlate and predict their biological activity. J Med Chem 37(24):4130–4146

Kumar R, Kumar A, Jain S, Kaushik D (2011) Synthesis, antibacterial evaluation and QSAR studies of 7-[4-(5-aryl-1,3,4-oxadiazole-2-yl)piperazinyl] quinolone derivatives. Eur J Med Chem 46(9): 3543–3550

Kurup A, Garg R, Hansch C (2000) Comparative QSAR analysis of 5alpha-reductase inhibitors. Chem Rev 100(3):909–924

Marberger M (2006) Drug Insight: 5alpha-reductase inhibitors for the treatment of benign prostatic hyperplasia. Nat Clin Pract Urol 3(9):495–503

McNicholas T, Mitchell S (2008) Benign prostatic hyperplasia. Surgery 26(5):218–222

Mittal RR, McKinnon RA, Sorich MJ (2009) The effect of molecular fields, lattice spacing and analysis options on CoMFA predictive ability. QSAR Comb Sci 28(6–7):637–644

Murumkar PR, Le L, Truong TN, Yadav MR (2011) Determination of structural requirements of influenza neuraminidase type A inhibitors and binding interaction analysis with the active site of A/H1N1 by 3D-QSAR CoMFA and CoMSIA modeling. Med Chem Comm 2(8):710–719

Parsons JK, Kashefi C (2008) Physical activity, benign prostatic hyperplasia, and lower urinary tract symptoms. Eur Urol 53(6): 1228–1235

Puntambekar D, Giridhar R, Yadav MR (2006) 3D-QSAR studies of farnesyltransferase inhibitors: a comparative molecular field analysis approach. Bioorg Med Chem Lett 16(7):1821–1827

Roehrborn CG, Siami P, Barkin J, Damião R, Becher E, Miñana B, Mirone V, Castro R, Wilson T, Montorsi F (2009) The influence of baseline parameters on changes in international prostate symptom score with dutasteride, tamsulosin, and combination therapy among men with symptomatic benign prostatic hyperplasia and an enlarged prostate: 2-Year data from the CombAT study. Eur Urol 55(2):461–471

SYBYL Molecular Modeling System (2003). Version 7.0

Thareja S, Aggarwal S, Bhardwaj TR, Kumar M (2009) Self organizing molecular field analysis on a series of human 5alpha-reductase inhibitors: unsaturated 3-carboxysteroid. Eur J Med Chem 44(12):4920–4925

Uemura M, Tamura K, Chung S, Honma S, Okuyama A, Nakamura Y, Nakagawa H (2008) Novel 5 alpha-steroid reductase (SRD5A3, type-3) is overexpressed in hormone-refractory prostate cancer. Cancer Sci 99(1):81–86